In-chair movements: Categorizations and patterns over time based on a literature review.

Kruithof, A; Song, YW; Vink, P

DOI
10.1177/10519815251394878

Licence
CC BY

Publication date
2025

Document Version
Final published version

Published in
Work (Reading, Mass.)

Citation (APA)
Kruithof, A., Song, YW., & Vink, P. (2025). In-chair movements: Categorizations and patterns over time based on a literature review. *Work (Reading, Mass.)*, *83*(1), 74-83. https://doi.org/10.1177/10519815251394878

3D Printing in Medicine

RESEARCH

Open Access

Facial 3D data acquisition in critically ill children for production of personalized non-invasive ventilation masks: a feasibility study

Rosemijne R. W. P. Pigmans[1,2*], Lyè Goto[3], Rens Wientjes[4], Dick G. Markhorst[1], Job B. M. van Woensel[1,2], Michael A. Gaytant[5], Toon Huysmans[3], Coen D. Dijkman[6] and Reinout A. Bem[1,2]

Abstract

Background Non-invasive ventilation is commonly used to support critically ill children with acute respiratory failure in the pediatric intensive care unit. However, non-invasive ventilation treatment is often hindered by poorly fitting masks due to limited commercially available options. Personalized non-invasive ventilation masks are a promising solution, yet research on the feasibility of their production in real-world clinical settings, particularly regarding facial data acquisition, remains limited. This study aims to assess the feasibility of using a handheld 3D scanner for facial data acquisition in critically ill children admitted to the pediatric intensive care unit.

Methods In this single-center pediatric intensive care unit feasibility study, facial 3D data was obtained from children (age 0–18 years) receiving non-invasive respiratory support for acute respiratory failure, using a handheld 3D scanner. Feasibility outcomes included the scan process and quality factors. Scan quality was evaluated based on scan errors and removed movement frames. Facial 3D data acquisition was defined as feasible if > 80% of patients had a complete scan whereof > 90% frames had a scan error < 0.5.

Results We included 33 patients with a median (IQR) age of 2.0 (1.0–16.0) months. Full facial 3D data could be acquired within a short scanning period of 30 s, which did not induce patient clinical deterioration, with a success rate of 31 (94%) usable scans with good quality (98% good frames).

Conclusion Our results show that facial data acquisition using a handheld 3D scanner is feasible in critically ill children receiving non-invasive respiratory support in the pediatric intensive care unit. These findings are essential for developing and implementing a workflow process for personalized non-invasive ventilation masks for children with acute respiratory failure.

Keywords 3D scanning & printing, Personalization, Respiratory support, Pediatric ICU, Acute respiratory failure

*Correspondence:
Rosemijne R. W. P. Pigmans
r.r.pigmans@amsterdamumc.nl
[1]Pediatric Intensive Care Unit, Emma Children's Hospital, Amsterdam UMC, Location AMC, University of Amsterdam, Amsterdam, The Netherlands
[2]Amsterdam Reproduction and Development Research Institute, Amsterdam UMC, University of Amsterdam, Amsterdam, The Netherlands
[3]Faculty of Industrial Design Engineering, Delft University of Technology, Delft, The Netherlands
[4]Directorate of Facility Management, University Medical Center Utrecht, Utrecht University, Utrecht, The Netherlands
[5]Center of Home Mechanical Ventilation, Department of Pulmonology, University Medical Center Utrecht, Utrecht University, Utrecht, The Netherlands
[6]Department MedTech Prototyping and Development, Amsterdam UMC, University of Amsterdam, Amsterdam, The Netherlands

Background

Non-invasive ventilation (NIV) is a frequently used treatment in critically ill children with acute respiratory failure admitted to the pediatric intensive care unit (PICU) [1, 2]. Yet, NIV in this setting is not always successful, necessitating intubation and invasive mechanical ventilation which is associated with additional harm [3, 4]. One of the major challenges of pediatric NIV, contributing to treatment failure, is obtaining a properly fitting interface [5, 6]. Commercially available pediatric NIV masks are currently limited in sizes and dimensions, posing an important risk factor for NIV failure, particularly in young children and those with specific facial features. To overcome this challenge, mask personalization is believed to be a promising future approach to improve pediatric NIV efficiency [5–13].

Several studies have investigated the assembly and/or performance of personalized masks for children in bench testing [11, 14, 15]. However, there is a scarcity of data that address the feasibility of the production and implementation process of such customized masks in a real-world acute clinical setting, such as the PICU. This also applies to facial data acquisition, which is a crucial first step in the production cycle of mask personalization. Handheld 3D scanners are currently advised for immobile patients, as these have high accuracy, reaching up to 0.1 mm, while being relatively quick with reported scanning times between 1 and 10 min [11, 16–19]. However, whether such handheld scanners can be used in the accurate facial data acquisition of critically ill, mobile children in need of respiratory support in the PICU is unknown.

The aim of this study is to examine the feasibility of facial data acquisition in critically ill patients admitted to the PICU for acute respiratory failure using a handheld 3D scanner. Knowledge derived from this study can be used to establish a clinical workflow for the rapid production of pediatric personalized NIV masks.

Methods

This was a single-center, feasibility study conducted in the PICU of the Emma Children's Hospital, Amsterdam UMC, Amsterdam, the Netherlands. The study was determined to not fall within the scope of the Medical Research Involving Human Subjects Act by the local research medical ethics board (W22_330#22.408). Informed consent for the use of data was obtained from the parents or caretakers. Recruitment and data collection took place from November 2022 to January 2025.

Subjects

The eligible study population consisted of all children (age 0–18 years) with acute respiratory failure admitted to the PICU receiving non-invasive respiratory support for > 2 h in the form of NIV (mode NIV/NIV-spontaneous timed, nasal continuous positive airway pressure (with pressure support)) on a Hamilton-G5 or Hamilton-C6 ventilator (Hamilton Medical, Bonaduz, Switzerland) using a conventional, commercially available face mask (total, oronasal or nasal) or had been switched to high flow nasal cannula (HFNC) treatment after an episode of NIV. Patients with chronic or acute-on-chronic respiratory failure already receiving NIV through their home ventilation machine and interface were excluded. We aimed for a sample size of 30–34 subjects for this feasibility study, based on the guidelines for designing and evaluating feasibility pilot studies [20]. We collected age, gender, height, weight, respiratory support mode, and settings at the moment of the scan, etiology of respiratory failure, and use of sedation as the patient characteristics.

Scanning protocol

A single trained observer scanned all the subjects using the structured light Artec Leo 3D scanner (Artec 3D, Luxembourg). This scanner has an accuracy of 0.1 mm and a data acquisition speed of 35 million points per second. The timing of the scan was planned together with the PICU nurses to select a moment for the 3D-scan to align with a routine mask change or caring moment. For this moment, patients were positioned on their back and remained in this position during scanning. The room lights were adjusted and the head was positioned in an upward position in order that the mouth-nose region could be scanned from one side of the bed, without the use of markers. When ready, the nurse removed the mask and the scan was made with a scanning distance of 0.7 m. A single scan was limited to a maximum of 30 s with a scanning speed of 60 frames per second and the function 'optimize project size', which only stores sufficiently novel captured frames with at least 3 frames per second, enabled [21]. Data is locally stored on the scanner under a study code, and displaced to a secured storage system. If the visual inspection of the resulting scan indicated missing data an additional scan was performed to ensure completeness. During scanning, the subjects continued to receive standard PICU monitoring of vital signs. In the case of patient agitation, clinical distress, or oxygen desaturation ($SpO_2 < 93\%$), the scan could be paused, postponed, or canceled and the non-invasive respiratory support was restarted, in accordance with the normal protocol during a routine mask change or caring moment. In none of the patients any residing nasogastric tubes were removed for the scan.

Post-processing

All scans were post-processed with the software accompanying the scanner (Artec Studio, Artec 3D, Luxembourg) in two ways: once by a manual process (manual method) and, alternatively, once using the autopilot

function. This function is a simplified form of post-processing which is more time efficient and objective, valuable for workflow development, but can have difficulties in successfully processing scans with movement. For both methods, first the surroundings were removed and frame alignment with global registration was performed. Next, for the manual process, the scans were examined per frame. The frames that contained evident facial expressions (e.g. frowning, talking, crying) were removed, and the remaining frames were grouped with similar head positions. Subsequently, the scans were manually aligned and after global registration and outlier removal, the scans were fused with smooth fusion with all holes smaller than 10 mm filled. For the autopilot method, the software reconstructed the faces automatically. If a first round of the autopilot function was not sufficient in creating a fusion, the function was repeated with a maximum of three tries. Additionally, the manual process was repeated for only the first scan of the sessions which required multiple scans (first scan method). Figure 1 provides an overview of the post-processing workflow.

Outcomes

Primary study outcomes were related to feasibility of scanning, including scanning process and quality factors. We predefined that facial data acquisition by a handheld 3D scanner in the PICU setting was considered feasible if > 80% of the patients can be successfully scanned in one session resulting in a complete scan with > 90% of the frames of good quality.

For the scanning process outcomes, we gathered information on patient clinical status, the need of scan postponement, and the number of scans per session and complete scans. Any event of patient clinical deterioration during scanning with the non-invasive respiratory support interface removed was noted. Scans were noted as scan postponement if the initiation needed to be delayed due to agitation, restlessness or a critical clinical situation. These patients were scanned at another occasion, within the next 24 h. The number of scans per session was collected as well as the reason for needing any additional scan (e.g. patient became agitated, moved, or the scan seemed incomplete). A scan was marked complete if there were no missing data, visible as holes, upon post-processing in the oronasal mask region. Incomplete scans with holes < 10 mm that could be filled, were marked as repairable. Finally, incomplete scans with holes > 10 mm were marked as unrepairable.

Scan quality outcome was assessed based on two categories: scan error and removed movement frames. Scan error is given by the scanners' post-processing software and is the parameter that reflects frame registration quality. Error values in the range of 0.0-0.5 are seen as good results, 0.6–1.3 as acceptable, and 1.4 or higher as

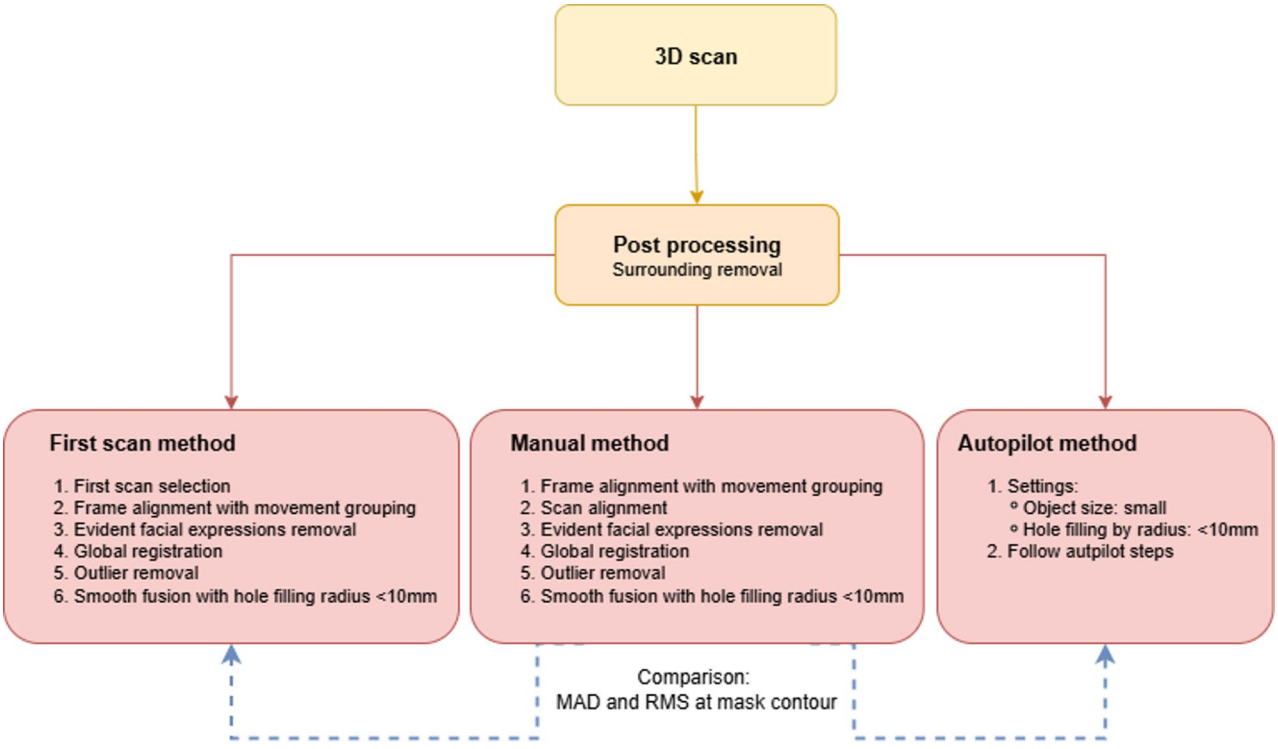

Fig. 1 The post-processing workflow overview. All scans are post-processed, with the first step being the surroundings removal. There are three different post-processing methods used: manual, autopilot, and first scan. The mean absolute distance (MAD) and root mean square (RMS) are defined by the software in a comparison between the mask regions of the manual method and both the first scan and the autopilot method

Table 1 Subject characteristics

Characteristics	*N* = 33
Age (months), median (IQR)	2.0 (1.0–16.0)
Gender (male), n (%)	21 (64)
Height (cm), median (IQR)	70.5 (55.0—111.5)
Weight (kg), median (IQR)	5.0 (4.3–8.8)
Receiving sedatives (yes), n (%)	22 (67)
Intravenous administration, n	6
Nasogastric tube (yes), n (%)	26 (79)
Non-invasive respiratory support mode, n (%)	
NIV	17 (52)
nCPAP(+PS)	9 (27)
HFNC	7 (21)
Reason for acute respiratory support, n	
Acute lower respiratory tract infection	24
Post-extubation	4
Other	2
FiO_2 (%), median (IQR)	30 (25–45)
PEEP[a] (cmH_2O), median (IQR)	6 (6–8)
ΔPinsp/PS[a] (cmH_2O), median (IQR)	10 (7–12)

[a] in patients receiving NIV or nCPAP + PS only. NIV: non-invasive ventilation; nCPAP(+PS): nasal continuous positive airway pressure with pressure support; FiO_2: fraction of inspired oxygen; PEEP: positive end-expiratory pressure; ΔPinsp/PS: pressure above PEEP

Table 2 Results on scanning feasibility (process and quality)

Scan characteristics	*N* = 33
Successful scan, n of patients (%)	31 (94)
Number of scans per patient, n of patients	
1	16
2	16
4	1
Reason additional scan needed (*n* = 17), n of patients	
Agitation	4
Patient movement	8
External interference	1
Incomplete scan	4
Total frames per patient, median (IQR)	75 (49–181)
Used frames per patient, median (IQR)	59 (41–117)
Percentage of frames with movement, median (IQR)	10 (0–35)
Completeness of scans, n of patients (%)	
Complete	14 (42)
Repairable	17 (52)
Unrepairable	2 (6)
Scan quality per frame (scan error), median (IQR)	
Good	98 (86–100)
Acceptable	2 (0–14)
Unusable	0 (0–0)

unusable [22]. These values are an internal parameter of Artec Studio and indicate the correct alignment in relation to each other [23]. The percentage of good, acceptable, and unusable frames was noted per scan. The percentage of removed movement frames is the number of removed frames during post-processing.

Finally, the mean absolute distance (MAD) and root mean square (RMS) between the manual method and the first scan method, and between manual method and the autopilot method were calculated at the oronasal mask contour (shown in Supplemental eFigure 1). Furthermore, the maximal absolute distance was calculated for the same comparisons and categorized into three groups: <1.0 mm, between 1.0 and 2.0 mm, and >2.0 mm. The maximal distance quantifies the deviation from the manual method, defined as the accurate depiction of the facial morphology, which would result in a misfit of a personalized mask. To minimize these post-processing errors, we chose strict distance categorizations.

Statistical analysis

All parameters were examined with explorative statistics using IBM SPSS Statistics (version 28). Results are reported as means (SD) or medians (IQR) where appropriate based on (non-)normal distributions.

Results

In total, 36 parents/guardians were approached for study participations and 33 patients were included. The patient characteristics of this cohort are shown in Table 1. The most common etiology of acute respiratory failure was lower respiratory tract infection. Most patients were receiving some form of (mild) sedation through enteral administration, and three patients received oral sucrose for soothing during their mask change or caring moment. NIV delivered by an oronasal or total face mask was the most common non-invasive respiratory support mode. A nasogastric tube was present in 26 (79%) patients and did not induce scanning artifacts.

Scanning characteristics and outcomes are summarized in Table 2. All 33 patients could be scanned without the need to cancel the session due to events of patient clinical deterioration during scanning (an example of a post-processed scan is shown in Fig. 2). Nevertheless, two patients were too agitated accompanied by a short period of oxygen desaturation at the start of the caring moment with the need to postpone the scanning process shortly. In two other patients, scanning needed to be postponed to another day due to a critical clinical situation and agitation of the patient during routine care before the start of the scanning session. A median (IQR) of 75 (49–181) frames were saved by the 'optimize project size' function per session whereof a median (IQR) of 10 (0–35)% of the frames had to be removed due to patient movement. After post-processing, the scans of two patients (6%) had unrepairable missing data, thus having an unsuccessful scanning attempt. Scans of 17 patients (52%) had repairable missing data. The scans of the remaining 14 patients had complete scanning frames.

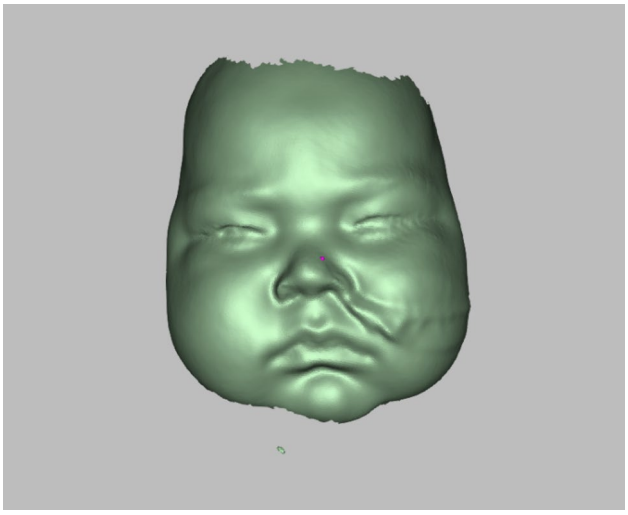

Fig. 2 Example of a high quality, manually post-processed, 3D scan of a patient. The scan can be saved as an .stl file. This scanning session contained a single, 30 s scan. The outline of a nasogastric tube fixed with tape at the left nostril can be observed

A total of 17 patients (52%) required an additional scanning period during the same session after the first try, whereof patient movement was the main reason in 8 (47%) patients. However, the additional scan did not induce a difference > 1.0 mm in 56% of patients (data shown in Supplemental eTable 1). There were no differences between the group with and without an additional scan regarding age, sedative use, ventilation pressure, FiO_2 or ventilator mode (data shown in Supplemental eTable 2). Only in the subgroup of four (23.5%) patients with multiple scans due to agitation, all additional scans improved the gathered information with differences > 1.0 mm. The median (IQR) MAD and RMS were 0.21 (0.10–0.40) and 0.28 (0.19–0.53), respectively. An example of the post-processing of a session with multiple scans, with head and facial movement, is shown in Fig. 3.

When using autopilot post-processing, the number of patients with an unrepairable scan was 4 (12%), as compared to the 2 patients with an unsuccessful attempt using the manual method. In these additional two patients, larger head deviation by movement caused the autopilot function to be insufficient (an example is shown in Fig. 3). The maximal distance between the two post-processing methods was < 1.0 mm in 18 scans, between 1.0 and 2.0 mm in 8 scans, and > 2.0 mm in 3 scans, with a MAD (IQR) of 0.11 (0.06–0.19) and a RMS (IQR) of 0.19 mm (0.10–0.30). The scan error value was considered good in 91% (IQR 65–99) of the frames, acceptable in 8%, and unusable in 1% (see Table 3).

Discussion

The main goal of this study was to evaluate the feasibility of acquiring facial 3D data in critically ill patients receiving non-invasive respiratory support for acute respiratory failure in the PICU. Our findings show that facial 3D data can be captured successfully within a very short period by a handheld scanner in more than 90% of patients in this setting, with good scanning quality in over 95% of the frames.

In the last decade, 3D scanning as a novel form of medical data acquisition, is a rapidly growing field [24, 25]. The applications of this method vary widely, from medical device adaptation to aiding diagnosis and treatment, regularly complemented with 3D printing [24, 26]. However, studies on 3D data capture and 3D printing for the purpose of personalized medical device development in critical care have been relatively scarce [27]. In our study cohort of critically ill patients one of the reasons for this is the potential difficulty of implementing a rapid, bedside, 3D-based scanning and printing process. Fortunately, the possibilities expand with the rise of handheld, wireless 3D scanners [24, 25] and 3D printing of (flexible) biocompatible materials [28–30]. Such advances are reported in several recent studies pertaining to various clinical care settings, including their use during facial surgery [31], burn injury wound mapping and tracking [32], and the production of artificial cardiac valves [33]. The current study contributes to this field by specifically testing 3D scanning feasibility in critically ill children for the development of personalized NIV masks. The combination of potential movement and the need for interrupting ongoing respiratory support to expose the face, in a patient category that is not instructible, creates an obvious barrier for accurate data capture. Previously, photogrammetry or even facial impressions were used for facial data acquisition in personalized ventilation mask production, limiting this application to clinically stable and mobile patients [17, 18, 34, 35]. Three recent studies looked into the 3D scanning of neonates for the development of nasal masks. However, one of these studies comprised a case report, in another study testing occurred in a simulated neonatal ICU setting, and the third study did not provide information on the actual feasibility in the clinical care setting [16, 36, 37]. With our study, we show that short scanning times with a handheld structured light 3D scanner are sufficient to capture high quality facial data in the PICU setting, even in the presence of movement. Previously, we have shown that such data can be used for the 3D printing of pediatric NIV masks [15]. These feasibility data are essential to further develop and implement a workflow process for the production of personalized NIV masks for children with acute respiratory failure. In addition, they are potentially relevant for other (medical device) applications in various acute clinical

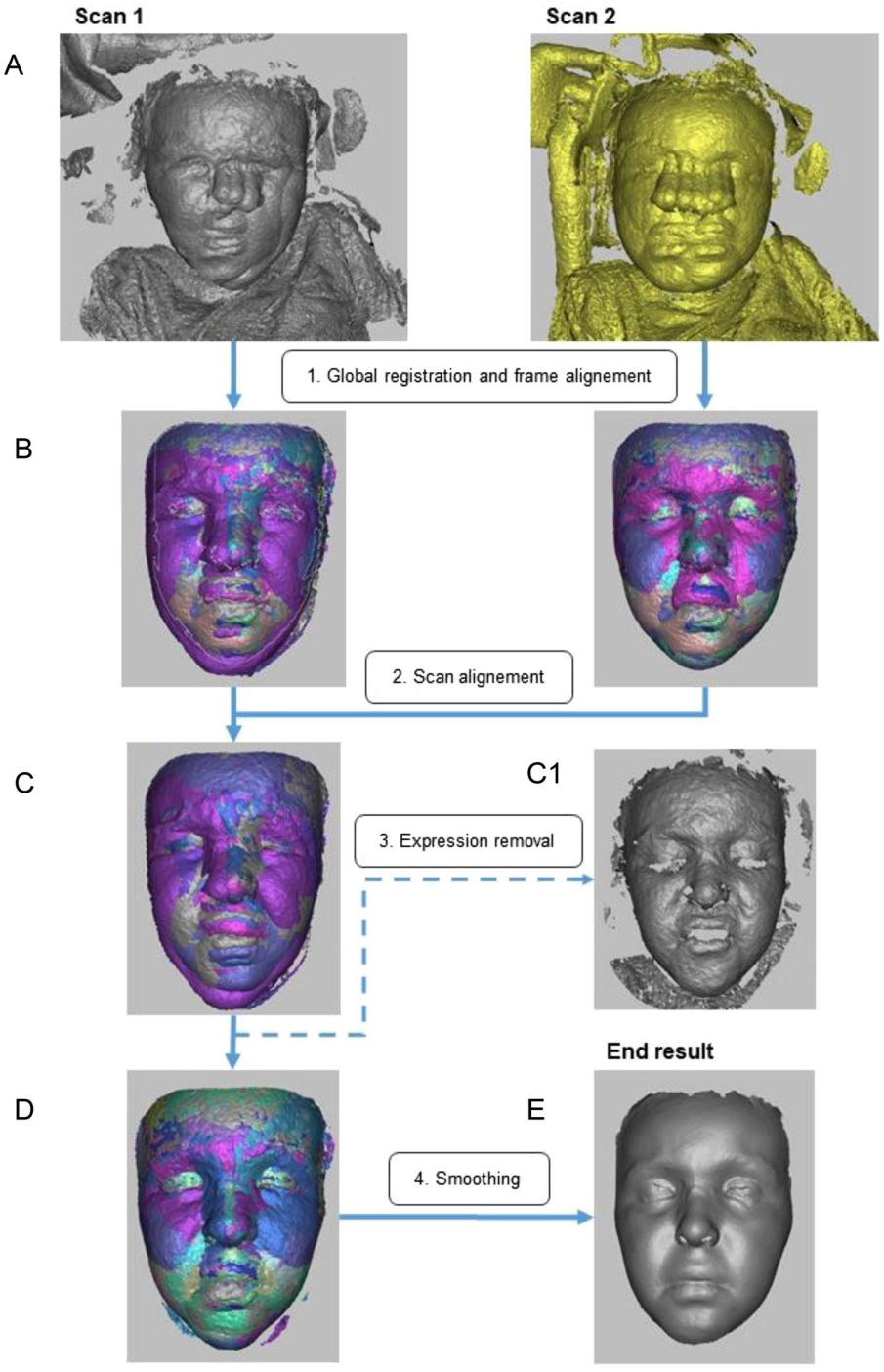

Fig. 3 Example of the post-processing steps in a session containing two separate scans. From top to bottom: (1) surroundings of scans A were removed, frames with similar head positions grouped (color-coded), and global registration performed; (2) Scans 1 and 2 of B were combined and aligned; (3) From combined scan C, facial expressions removed, an example of removed facial expressions is shown in C1; and (4) remaining frames of scan D were fused into scan E. During the first scan, agitation caused head movement and facial expressions. Efficient post-processing using the Artec Studio Autopilot function was not feasible in this case

care settings in the hospital, including the ICU and the emergency room.

The number of successful scans in our study was higher than anticipated. Although in 58% of cases a second scan was performed, more than half did not provide relevant additional geometric information. Moreover, the median of 75 frames per scan, indicates that most scans were deemed sufficient before the 30 s threshold (90-1800

Table 3 Results for the frame quality using the Artec Studio autopilot function

Autopilot	***N*=33**
Quality autopilot (%)[a]	
Good	91 (65–99)
Acceptable	8 (1–31)
Unusable	1 (0–4)
Successful execution, n(%)	29 (88%)
Comparison with manual	***N*=29**
MAD (mm), median (IQR)	0.11 (0.06–0.19)
RMS (mm), median (IQR)	0.19 (0.10–0.30)
Max difference with manual method	
< 1.0 mm	18 (62)
1.0–2.0 mm	8(28)
> 2.0 mm	3(10)

MAD: mean absolute distance, RMS: root mean square

frames) was reached. The 25% IQR of 49 frames indicates scanning time of even 15 s to be sufficient. Therefore, we conclude that with sufficient training, the average scanning time needed to obtain an accurate, high quality facial scan can be lowered to a maximum of 30 s. In this study, all scans were performed by a single observer. However, the Artec Leo has been scored as user-friendly by clinicians, where a training time of less than 5 scans was necessary to obtain performer confidence and quality scans [36]. This suggests that the 3D scans could be performed by the clinical staff, improving workflow and time management. Nevertheless, the post-processing of the scan requires more time and expertise. During the scanning period, no clinically relevant adverse events occurred, and only a small portion (10%) of the frames needed removal due to movement. The resulting scans contained enough geometric data for reconstruction, deeming this technique feasible even for critically ill children in need of non-invasive respiratory support. Here, it is relevant to note that a large part of the children were receiving intermittent sedative medication to help tolerate their non-invasive respiratory support. In total, 18% of the population received continuous intravenous medication for sedation, as is commonly observed in NIV treatment in the PICU [3]. This will likely have had a dampening effect on patient movements and thus positively influenced our success rate of scanning. Besides movement, the nasogastric tube was expected to be a source of artifacts due to its translucent material. In our cohort, a nasogastric tube was present in almost 80% of the patients as standard practice for enteral feeding during NIV [38]. They are known to contribute to air leakage during NIV [39]. Recent studies indicate that modifying ventilation masks to accommodate the presence of nasogastric tubes can substantially reduce air leakage in commercial masks [40, 41]. In our study, presence of a nasogastric tube did not result in failed scans, which could facilitate the integration of geometric tube data into the design of personalized masks, potentially further enhancing NIV efficiency. However, whether the current scanning method is sufficient to facilitate adequate information for tube integration should be further investigated.

There are various techniques for 3D scanning patients and they have become more easily accessible in recent years [24, 42–45]. While the Artec Leo is often mentioned as one of the best options for handheld 3D scanning [17, 36, 46, 47], cheaper options are undergoing refinement and therefore increasingly used. A well-known example is the iPhone (LiDAR and TrueDepth function), which allows for easy and accurate scanning [16, 36, 42, 48]. A major limitation of these functions, however, is the lack of clear data protection regulations. Furthermore, an advantage of more professional scanners is the accompanying software, which improves the possibilities of post-processing [42]. The autopilot function of Artec Studio is one such advantage, improving the objectivity of post-processing steps and reducing the time needed. We showed that almost 80% of the scans could be post-processed immediately with this function, with a minimal MAD compared to manual post-processing. While manual processing could take up to an hour, the autopilot method mostly took around 15 min. The objectivity and reduction in time would be very useful for process implementation. For optimal use of the function, we advise removing frames with outspoken facial expressions before using the autopilot function for performance improvement.

A first limitation of this study is the absence of a control method to obtain 3D data of the patient, to compare the accuracy with the handheld scanner. However, it was deemed unethical to obtain more measurements in this group, as other scanning options are impractical for immobile patients or too time consuming for the critically ill patient in the PICU setting. Moreover, the accuracy of the Artec Leo has previously been shown to be extremely precise [36, 46]. In addition, our captured 3D data by this scanner was found of high quality, and easily to be loaded in our semi-automated software application as described before [15]. A second limitation is the timing of the scans, as we were not able to scan the patients within the first few hours of NIV, which in a clinical workflow for mask personalization would be desirable to ensure quick mask production and thus adequate NIV treatment. This was not feasible in the current study as consent for data acquisition was necessary from the parents. Yet, at this point, patients were still receiving a high level of respiratory support. As such, we do not believe this affected the feasibility of facial 3D data acquisition in a meaningful way. A third limitation, is that the categories of the maximal absolute distance to compare scan

post-processing methods were chosen semi-arbitrary. Currently, there is limited knowledge that helps characterize maximal allowable distances between masks and between masks and the facial region of interest to define an acceptable mask fit. The influence on mask performance by any distance (misfit) is highly dependent on materials, skin characteristics, and NIV settings. Visscher et. al. [6], showed that even small distances of a few mm are associated with skin erythema in children receiving NIV treatment. Moreover, the orifice flow equation, based on Bernoulli's principle, suggests that gaps/holes of only 2 mm already results in a substantial and clinically relevant leak air flow of 5 L/min at a peak amplitude pressure of 10 cmH_2O of ventilation, while a hole of 1 mm will result in an air leak flow of 1 L/min. For this reason, we choose the ranges for the maximal absolute distance quite strict to strive for the most optimal setting in terms of geometric fit. Lastly, as a fourth limitation, it should be noted that facial morphology depends on position [49, 50], and may influence mask fit. During the use of total and full face masks at the PICU, patients typically remain in a supine position. Therefore, we recommend to make the 3D scan of the patient in this position. A recent study [49] shows higher age and body fat to increase the change in morphology, probably limiting the gravitational effect in our population. Nevertheless, the exact influence of patient position and movement on the mask fit should be explored in a clinical study.

In conclusion, facial 3D data capture of critically ill patients receiving non-invasive respiratory support for acute respiratory failure in the PICU, by using a handheld structured light scanner, is feasible. This finding is crucial for the implementation of a production workflow for personalized NIV masks for children in this setting.

Abbreviations

FiO_2	Fraction of inspired oxygen
HFNC	High flow nasal cannula
MAD	Mean absolute distance
nCPAP(+PS)	Nasal continuous positive airway pressure (with pressure support)
NIV(-ST)	Non-invasive ventilation (spontaneous timed)
PEEP	Positive end-expiratory pressure
PICU	Pediatric intensive care unit
Pinsp	Inspiratory pressure above PEEP
RMS	Root meat square

Supplementary Information

The online version contains supplementary material available at https://doi.org/10.1186/s41205-025-00311-9.

Supplementary Material 1

Acknowledgements
We want to thank all parents and patients for contributing to this research.

Author contributions
RP: conceptualization, methodology, data collection, statistical analysis, writing and editing draft. LG: editing draft. RW: editing draft. DM: conceptualization, methodology, editing draft. MG: editing draft. JvW: editing draft. TH: editing draft. CD: conceptualization, methodology, editing draft. RB: conceptualization, methodology, editing draft.

Funding
This research is funded by the Innovation Award Amsterdam UMC, the Emma Children's Hospital Foundation, the Cornelia Foundation, Vermas Foundation, and NWO (Grant ID https://doi.org/10.61686/XFSHL93482).

Data availability
The datasets used and/or analyzed during the current study are available from the corresponding author on reasonable request.

Declarations

Ethics approval and consent to participate
The study was determined to not fall within the scope of the Medical Research Involving Human Subjects Act by the research medical ethics board of the Amsterdam UMC, Amsterdam (W22_330#22.408).

Consent for publication
Written informed consent for publication of their clinical images was obtained from the parents/guardians of the patients. A copy of the consent form is available for review by the Editor of this journal.

Competing interests
The authors declare no competing interests.

Received: 15 March 2025 / Accepted: 17 November 2025
Published online: 27 November 2025

References

1. Emeriaud G, Pons-Odena M, Bhalla AK, Shein SL, Killien EY, Modesto IAV, et al. Noninvasive ventilation for pediatric acute respiratory distress syndrome: experience from the 2016/2017 pediatric acute respiratory distress syndrome incidence and epidemiology prospective cohort study. Pediatr Crit Care Med. 2023. https://doi.org/10.1097/PCC.0000000000003281.
2. Mayordomo-Colunga J, Pons-Òdena M, Medina A, Rey C, Milesi C, Kallio M, et al. Non-invasive ventilation practices in children across Europe. Pediatr Pulmonol. 2018. https://doi.org/10.1002/ppul.23988.
3. Bermúdez-Barrezueta L, Mayordomo-Colunga J, Miñambres-Rodríguez M, Reyes S, Valencia-Ramos J, Lopez-Fernandez YM, et al. Implications of sedation during the use of noninvasive ventilation in children with acute respiratory failure (SEDANIV Study). Crit Care. 2024. https://doi.org/10.1186/s13054-024-04976-2.
4. Toni F, Cambra Lasaosa FJ, Conti G, Escuredo L, Benito S, Gelabert G, et al. Comparison in the management of respiratory failure due to bronchiolitis in a pediatric ICU between 2010 and 2016. Respir Care. 2019. https://doi.org/10.4187/respcare.06608.
5. Barker N, Willox M, Elphick H. A review of the Benefits, challenges and the future for interfaces for long term Non-Invasive ventilation in children. Int J Respir Pulm Med. 2018. https://doi.org/10.23937/2378-3516/1410077.
6. Visscher MO, White CC, Jones JM, Cahill T, Jones DC, Pan BS. Face masks for noninvasive ventilation: Fit, excess skin Hydration, and pressure ulcers. Respir Care. 2015. https://doi.org/10.4187/respcare.04036.
7. Brill AK, Pickersgill R, Moghal M, Morrell MJ, Simonds AK. Mask pressure effects on the nasal Bridge during short-term noninvasive ventilation. ERJ Open Res. 2018. https://doi.org/10.1183/23120541.00168-2017.
8. Wu YY, Acharya D, Xu C, Cheng B, Rana S, Shimada K. Custom-Fit Three-Dimensional-Printed bipap mask to improve compliance in patients requiring Long-Term noninvasive ventilatory support. J Med Device. 2018. https://doi.org/10.1115/1.4040187.
9. Hovenier R, Goto L, Huysmans T, van Gestel M, Klein-Blommert R, Markhorst D, et al. Reduced air leakage during Non-Invasive ventilation using a simple anesthetic mask with 3D-Printed adaptor in an anthropometric based

pediatric Head-Lung model. Front Pediatr. 2022. https://doi.org/10.3389/fped.2022.873426.
10. Fedor KL. Noninvasive respiratory support in infants and children. Respir Care. 2017. https://doi.org/10.4187/respcare.05244.
11. Bockstedte M, Xepapadeas AB, Spintzyk S, Poets CF, Koos B, Aretxabaleta M. Development of personalized Non-Invasive ventilation interfaces for neonatal and pediatric application using additive manufacturing. J Pers Med. 2022. https://doi.org/10.3390/jpm12040604.
12. Simpson R, Pascoe JE, Letcher J, Lin CY, Van Aalst J, Rulong GW, et al. editors. Customized, 3D-Printed nasal masks for the delivery of noninvasive positive airway pressure in patients with obstructive sleep apnea. Preliminary Findings: American Thoracic Society; 2020.
13. Morrison RJV, Kyle K, Nasser HB, Kashlan KN, Kline, Stephanie K, Jensen DR, Edwards SP, Hassen F, Schotland HM, Chervin RD, Buchman SR, Hollister SJ, Garetz SL, Green GE. Personalized 3D-printed CPAP masks improve CPAP effectiveness in children with OSA and craniofacial anomalies. Combined Otolaryngology Spring Meetings; Boston, MA2015.
14. Willox M, Metherall P, Jeays-Ward K, McCarthy AD, Barker N, Reed H, et al. Custom-made 3D printed masks for children using non-invasive ventilation: a feasibility study of production method and testing of outcomes in adult volunteers. J Med Eng Technol. 2020. https://doi.org/10.1080/03091902.2020.1769759.
15. Pigmans RRWP, Klein-Blommert R, Van Gestel MC, Markhorst DG, Hammond P, Boomsma P, et al. Development of personalized non-invasive ventilation masks for critically ill children: a bench study. Intensive Care Med Experimental. 2024. https://doi.org/10.1186/s40635-024-00607-w.
16. Kamath AA, Kamath MJ, Ekici S, Stans AS, Colby CE, Matsumoto JM, et al. Workflow to develop 3D designed personalized neonatal CPAP masks using iPhone structured light facial scanning. 3D print med. 2022. https://doi.org/10.1186/s41205-022-00155-7.
17. Willox M, Metherall P, McCarthy AD, Jeays-Ward K, Barker N, Reed H, et al. Custom-made 3D printed masks for children using non-invasive ventilation: a comparison of 3D scanning technologies and specifications for future clinical service use, guided by patient and professional experience. J Med Eng Technol. 2021. https://doi.org/10.1080/03091902.2021.1921869.
18. Pigmans RRWP, Smith JM, Markhorst DG, Van Woensel JBM, Dijkman CD, Elphick HE, et al. Current advances and gaps in knowledge on personalizing masks for non-invasive respiratory support: a scoping review. Respir Care. 2024. https://doi.org/10.4187/respcare.11886.
19. Artec Leo: Artec 3D. https://www.artec3d.com/portable-3d-scanners/artec-leo. Accessed 3 aug 2025.
20. Teresi JA, Yu X, Stewart AL, Hays RD. Guidelines for designing and evaluating feasibility pilot studies. Med Care. 2022. https://doi.org/10.1097/mlr.0000000000001664.
21. Settings. Scanning settings: Artec 3D; https://docs.artec-group.com/leo_/1.8/settings.html#scanning-settings. Accessed 11 mar 2025.
22. Data Processing. Maximum Error and Registration Quality: Artec Studio 16; https://docs.artec-group.com/as/16/en/process.html. Accessed 12 jun 2024.
23. Max error/Quality value in the Artec Studio Workspace. Artec 3D support center; https://support.artec3d.com/hc/en-us/articles/203700022-Max-error-Quality-value-in-the-Artec-Studio-Workspace. Accessed 19 jun 2025.
24. Haleem A, Javaid M. 3D scanning applications in medical field: A literature-based review. Clin Epidemiol Global Health. 2019. https://doi.org/10.1016/j.cegh.2018.05.006.
25. Wakjira Y, Kurukkal NS, Lemu HG. Reverse engineering in medical application: literature review, proof of concept and future perspectives. Sci Rep. 2024. https://doi.org/10.1038/s41598-024-74176-z.
26. Diment LE, Thompson MS, Bergmann JHM. Clinical efficacy and effectiveness of 3D printing: a systematic review. BMJ Open. 2017. https://doi.org/10.1136/bmjopen-2017-016891.
27. Boshra M, Godbout J, Perry JJ, Pan A. 3D printing in critical care: a narrative review. 3D printing in medicine. 2020. https://doi.org/10.1186/s41205-020-00081-6
28. Bachtiar EO, Erol O, Millrod M, Tao R, Gracias DH, Romer LH, et al. 3D printing and characterization of a soft and biostable elastomer with high flexibility and strength for biomedical applications. J Mech Behav Biomed Mater. 2020. https://doi.org/10.1016/j.jmbbm.2020.103649.
29. Borras-Novell C, Causapie MG, Murcia M, Djian D, Garcia-Algar O. Development of a 3D individualized mask for neonatal Non-Invasive ventilation. Int J Bioprint. 2022. https://doi.org/10.18063/ijb.v8i2.516.
30. Xu S, Ahmed S, Momin M, Hossain A, Zhou T. Unleashing the potential of 3D printing soft materials. Device. 2023. https://doi.org/10.1016/j.device.2023.100067.
31. Koban KC, Perko P, Etzel L, Li Z, Schenck TL, Giunta RE. Validation of two handheld devices against a non-portable three-dimensional surface scanner and assessment of potential use for intraoperative facial imaging. J Plast Reconstr Aesthetic Surg. 2020. https://doi.org/10.1016/j.bjps.2019.07.008.
32. Furferi R, Governi L, Pinzauti E, Profili A, Puggelli L, Volpe Y. A computational method for the investigation of burn scars topology based on 3D optical scan. Comput Biol Med. 2022. https://doi.org/10.1016/j.compbiomed.2022.105945.
33. Vernon MJ, Mela P, Dilley RJ, Jansen S, Doyle BJ, Ihdayhid AR, et al. 3D printing of heart valves. Trends Biotechnol. 2024. https://doi.org/10.1016/j.tibtech.2023.11.001.
34. Reddy NR, Sasikala N, Karthik K, Priya GK. Customized nasal prosthesis in continuous positive airway pressure treatment, current trend in treating obstructive sleep apnea for better patient compliance. J Family Med Prim Care. 2019. https://doi.org/10.4103/jfmpc.jfmpc_473_19.
35. Lanza CRM, de Arruda JAA, Soares AM, de Oliveira Santos M, de Souza AF, Lanza LD, et al. Fabrication of a custom pediatric nasal mask for noninvasive ventilation using a maxillofacial elastomer: A straightforward technique. J Prosthet Dent. 2019. https://doi.org/10.1016/j.prosdent.2018.02.017.
36. August D, Byram I, Forrestal D, Desselle M, Stevenson N, Iyer K, et al. Assessing the feasibility of handheld scanning technologies in neonatal intensive care: Trueness, acceptability, and suitability for personalised medical devices. Australian Crit Care. 2024. https://doi.org/10.1016/j.aucc.2024.09.012.
37. Martin-Gonzalez A, de la Morras B, Bergon-Sendin E, Jesus Perez-Lopez A, Ferrando-Sanchez A, Pallas-Alonso CR, et al. Feasibility of three-dimensional nasal imaging and printing in producing customized nasal masks for non-invasive ventilation in extremely low birth weight infant: A pilot study. Int J Bioprint. 2023. https://doi.org/10.18063/ijb.v9i1.627.
38. Viner Smith E, D'Cruz RF, Chapple L-A. Nutrition therapy during noninvasive ventilation: oral or enteral? Curr Opin Crit Care. 2023. https://doi.org/10.1097/mcc.0000000000001053.
39. Brill A-K. How to avoid interface problems in acute noninvasive ventilation. Breathe. 2014. https://doi.org/10.1183/20734735.003414.
40. Quintero OI, Sanchez AI, Chavarro PA, Casas IC, Ospina Tascón GA. Impact of using a novel gastric feeding tube adaptor on patient's comfort and air leaks during Non-invasive mechanical ventilation. Arch Bronconeumol. 2020. https://doi.org/10.1016/j.arbres.2019.10.002.
41. So EC, Chen Y-H, Wong K-L, Poon PW-F, Huang B-M. A new mask designed for patients implanted with a nasogastric tube. Med Eng Phys. 2008. https://doi.org/10.1016/j.medengphy.2007.09.007.
42. Wersenyi G, Scheper V, Spagnol S, Eixelberger T, Wittenberg T. Cost-effective 3D scanning and printing technologies for outer ear reconstruction: current status. Head Face Med. 2023. https://doi.org/10.1186/s13005-023-00394-x.
43. Petrides G, Clark JR, Low H, Lovell N, Eviston TJ. Three-dimensional scanners for soft-tissue facial assessment in clinical practice. J Plast Reconstr Aesthetic Surg. 2021. https://doi.org/10.1016/j.bjps.2020.08.050.
44. Mai H-N, Kim J, Choi Y-H, Lee D-H. Accuracy of portable face-Scanning devices for obtaining Three-Dimensional face models: A systematic review and Meta-Analysis. Int J Environ Res Public Health. 2020. https://doi.org/10.3390/ijerph18010094.
45. Mai H-N, Lee D-H. Accuracy of mobile Device–Compatible 3D scanners for facial digitization: systematic review and Meta-Analysis. J Med Internet Res. 2020. https://doi.org/10.2196/22228.
46. Spears SDJ, Lester T, Torii R, Kalaskar DM. Comparative evaluation of artec Leo hand-held scanner and iPad pro for 3D scanning of cervical and craniofacial data: assessing precision, accuracy, and user experience. 3D printing in medicine. 2024. https://doi.org/10.1186/s41205-024-00245-8.
47. Kropla F, Winkler D, Lindner D, Knorr P, Scholz S, Grunert R. Development of 3D printed patient-specific skull implants based on 3d surface scans. 3D printing in medicine. 2023. https://doi.org/10.1186/s41205-023-00183-x.
48. Alhazmi B, Alshomer F, Alazzam A, Shehabeldin A, Almeshal O, Kalaskar DM. Digital workflow for fabrication of bespoke facemask in burn rehabilitation with smartphone 3D scanner and desktop 3D printing: clinical case study. 3D Print Med. 2022. https://doi.org/10.1186/s41205-022-00140-0.
49. Thottungal RR, Harnádková K, Dupej J, Velemínská J. Gravity's influence on facial shape changes during vertical and horizontal head scanning: effects of sex, age, and body fat. Forensic Sci Int. 2025. https://doi.org/10.1016/j.forsciint.2025.112516.

50. Munn L, Stephan CN. Changes in face topography from supine-to-upright position—And soft tissue correction values for craniofacial identification. Forensic Sci Int. 2018. https://doi.org/10.1016/j.forsciint.2018.05.016.

Publisher's note